Carbohydrate Polymers 98 (2013) 1179–1185

Contents lists available at ScienceDirect

Carbohydrate Polymers

journal homepage: www.elsevier.com/locate/carbpol

Effect of methylcellulose on the formation and drug release behavior of silk fibroin hydrogel

Cho Hee Park[a], Lim Jeong[a], Donghwan Cho[b], Oh Hyeong Kwon[b], Won Ho Park[a,*]

[a] Department of Advanced Organic Materials and Textile System Engineering, Chungnam National University, Daejeon 305-764, South Korea
[b] Department of Polymer Science and Engineering, Kumoh Institute of Technology, Kumi-City 730-701, South Korea

ARTICLE INFO

Article history:
Received 14 May 2013
Received in revised form 5 July 2013
Accepted 10 July 2013
Available online 18 July 2013

Keywords:
Silk fibroin
Methylcellulose
Gelation
Drug release

ABSTRACT

In this study, methylcellulose (MC) was used to control the gelation time of silk fibroin (SF) aqueous solution. The gelation time was measured using a Vibro Viscometer at 50 °C. Fourier transform infrared spectroscopy (FT-IR), scanning electron microscopy (SEM), and a texture meter were used to investigate the effect of MC on the hydrogelation of SF solution. SF/MC hydrogels could be formed by the addition of MC, although their gelation time was increased with MC content. To examine the conformational change of SF/MC hydrogels, time-resolved FT-IR spectra were obtained at constant temperature using a custom-made IR chamber. From FT-IR spectra focused on the amide I peak position, the transition of SF molecules in SF/MC solution from a random coil to a β-sheet structure was inhibited in the presence of MC molecules. In addition, the drug release of SF/MC hydrogels loaded with 5-aminosalicylic acid was studied in 2-dimensional (2-D) and 3-dimensional (3-D) conditions *in vitro*. The drug release behavior of SF or SF/MC hydrogels was measured using UV–Vis spectroscopy. The release rate of 5-aminosalicylic acid in SF/MC hydrogel was lower than that of SF hydrogel, which may be closely associated with the hydrophilic interaction between MC and 5-aminosalicylic acid. This approach to controlling the sol–gel transition and the drug release of SF hydrogels by the addition of MC will be useful in the design and tailoring of novel materials for biomedical applications.

1. Introduction

Hydrogels are chemically or physically crosslinked 3-D polymer networks with high water content (Lee & Mooney, 2001). Hydrogel has excellent biocompatibility due to the high water content and the nature of the polymer. Therefore, hydrogels are widely used in various biomedical applications, such as drug delivery systems, contact lenses, encapsulation materials for immunoisolation-based cell therapeutics, wound dressings, and tissue engineered scaffolds (West & Hubbell, 1995; Wang, Kluge, Leisk, & Kaplan, 2008; Vos et al., 2009; Kundu, Poole-Warren, Martens, & Kundu, 2012).

Silk is a natural fibrous protein that is spun into fiber by silkworms and spiders. Silkworm silk primarily consists of two protein components: fibroin and sericin. The pure fibroin component can be obtained by removing sericin using various degumming conditions. Regnerated SF can be fabricated in various forms, such as gels, powders, fibers, and membranes (Li et al., 2002; Shang, Zhu, & Fan, 2011; Yao, Masuda, Zhao, & Asakura, 2002; Putthanarat et al., 2002; Ayutsede et al., 2005; Jin & Kaplan, 2003). SF has been widely used for cosmetics and food additives, and has recently been found to have potential in the areas of biomedical science and engineering due to its distinctive biological properties (Padamwar & Pawar, 2004; Fuji, Takahashi, & Kinouchi, 2000; Motta, Migliaresi Lloyd, Denyer, & Santin, 2002; Motta et al., 2004). SF has attracted much attention for its biocompatibility, oxygen and water vapor permeability, biodegradability, and minimal inflammatory reactions *in vitro* (Sakabe, Ito, Miyamoto, Noishiki, & Ha, 1989; Park et al., 2001; Santin, Motta, Freddi, & Cannas, 1999). Due to these biological properties, SF is promising as a scaffolding material for tissue engineering. It was previously reported that SF matrices could be useful for the culture of fibroblasts, osteoblasts and stem cells, and could enhance the adhesion, growth, and differentiation of the cells in a manner similar to that of collagen matrices (Cai, Yao, Cui, et al., 2002; Cai, Yao, Lin, et al., 2002; Min, Jeong, et al., 2004; Karageorgiou et al., 2004).

It is known that the hydrogelation of SF is accompanied by a conformational transition from a random coil to a β-sheet structure in the sol (Matsumoto et al., 2006; Kim et al., 2004). Various studies have accomplished the variation of the sol–gel transition of SF solution. The gelation rate of SF solution can be adjusted by

* Corresponding author at: Department of Textile Engineering, College of Engineering, Chungnam National University, Daejeon 305-764, South Korea.
Tel.: +82 42 821 6613; fax: +82 42 823 3736.
E-mail address: parkwh@cnu.ac.kr (W.H. Park).

0144-8617/$ – see front matter © 2013 Elsevier Ltd. All rights reserved.
http://dx.doi.org/10.1016/j.carbpol.2013.07.028

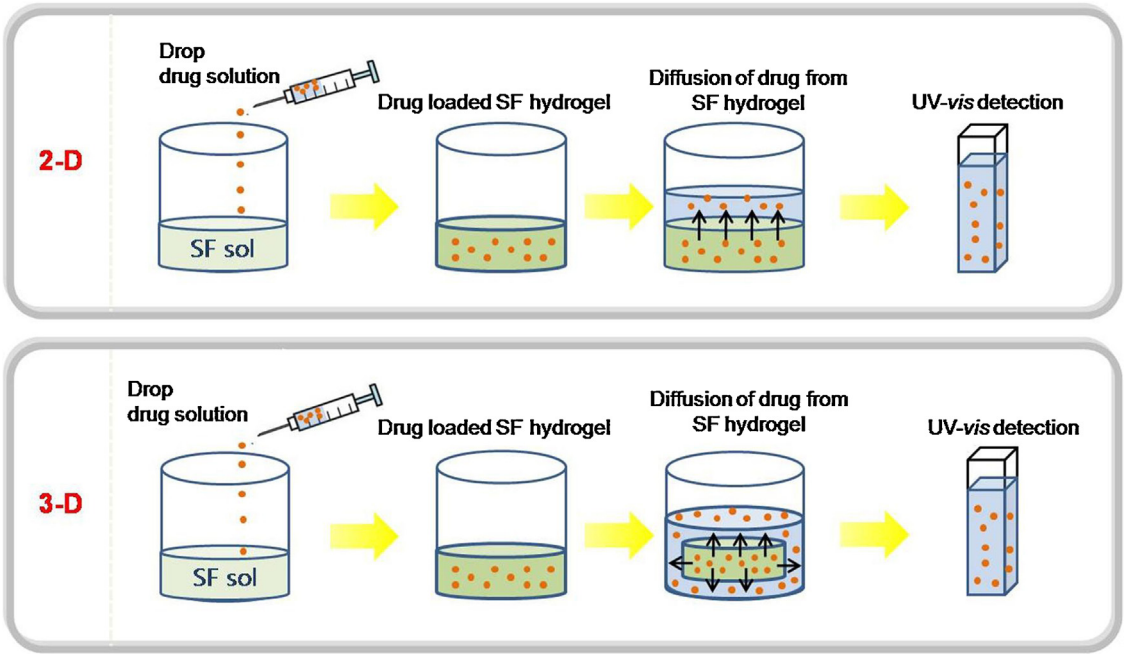

Scheme 1. Schematic diagram of drug release (2-, 3-dimensions) in SF hydrogel.

changing physical or chemical conditions such as concentration, temperature, and pH (Matsumoto et al., 2006; Kim et al., 2004). Additives such as salts, metal ions, and surfactants are known to accelerate the sol–gel transition of SF aqueous solution (Kim et al., 2004; Wu et al., 2012). SF can be blended with various synthetic or natural polymers to improve either the properties of hydrogel or to shorten the gelation rate (Yoo, Kweon, Lee, Lee, & Cho, 2004; Gil, Frankowski, Spontak, & Hudson, 2005; Lv, Hu, Feng, & Cui, 2008; Dinerman, Cappello, Ghandehari, & Hoag, 2002; Mandal, Kapoor, & Kundu, 2009).

MC is a hydrophilic cellulose derivative obtained by methylation using chloromethane. MC is widely used as a binding or thickening additive in the pharmaceutical, cosmetic, and food industries due to its temperature-sensitive behavior. The gelation behavior of MC aqueous solution is unique in terms of temperature-related inverse solubility (Lin, Wang, Wei, & Li, 2007). The gelation temperature of MC is strongly dependent on the ratio of hydrophobic moiety to hydrophilic moiety in the MC backbone (Hirrien, Chevillard, Desbrieres, Axelos, & Rinaudo, 1998; Arisz, Kauw, & Boon, 1995).

We report on the effect of MC on the gelation of SF aqueous solution and the release behavior of drug-loaded SF hydrogels. The conformational changes of the SF solution during the gelation, with or without MC, were investigated by time-resolved FT-IR spectra. In addition, the drug release of SF and SF/MC hydrogels was studied using 5-aminosalicylic acid as a model drug. In order to investigate the effect of MC on the drug release from hydrogels, the 2-D and 3-D drug release behavior of SF or SF/MC hydrogels was compared using UV–Vis spectroscopy.

2. Experimental

2.1. Materials

Raw 12-denier silk fibers (*B. mori*) were supplied by Daejeon Sangsa Co., Korea. MC (DS = 1.6–1.9) and 5-aminosalicylic acid (mesalamine) (MW 151 Da) were purchased from Sigma–Aldrich Co., and used without further purification.

2.2. Preparation of regenerated SF solution

Degummed silk yarn was dissolved in a ternary solvent system composed of calcium chloride, ethanol, and water (1:2:8 molar ratio) at 70 °C for 4 h, followed by dialysis with cellulose tubular membranes (250–7 μ, Sigma Co.) against distilled water for 3 days (Min, Lee, et al., 2004). The dialyzed SF solution was centrifuged to remove the insoluble residues, and the final concentration of the resultant SF solution was approximately 2.0 wt%.

2.3. Preparation of SF/MC solution

1 g of MC powder was dispersed in 50 mL of distilled water at 90 °C, and then cooled down and kept at room temperature for 6 h with stirring to prepare a clear MC solution (2 wt%). MC solution was mixed with SF solution (2 wt%) under stirring in blending ratios of 100/0, 70/30, 50/50, and 30/70 (v/v) for a specified period of time.

2.4. Gelation of SF/MC solution

The gelation behavior of pure SF solution was examined at room temperature, 37 °C and 50 °C. The gelation time was determined when the sample did not flow from an inverted vial within 30 s (Kim et al., 2004). The gelation of SF/MC solution was observed at 50 °C.

2.5. Drug release

1 mL of 5-aminosalicylic acid solution (10 mM in phosphate buffered saline (PBS) at pH 7.2) was added to 30 mL of SF solution or SF/MC solution (MC content: 0%, 30%, 50%, and 70% in volume ratio). SF and SF/MC hydrogels loaded with 5-aminosalicylic acid were then prepared at 37 °C and 50 °C, respectively. Drug release was investigated by adding 50 mL of PBS (pH 7.2) to SF hydrogel or SF/MC hydrogel in 2-D and 3-D conditions, as shown in Scheme 1. Drug release (%) was determined using a UV–Vis spectrophotometer (UV-2450, Shimadzu, Japan).

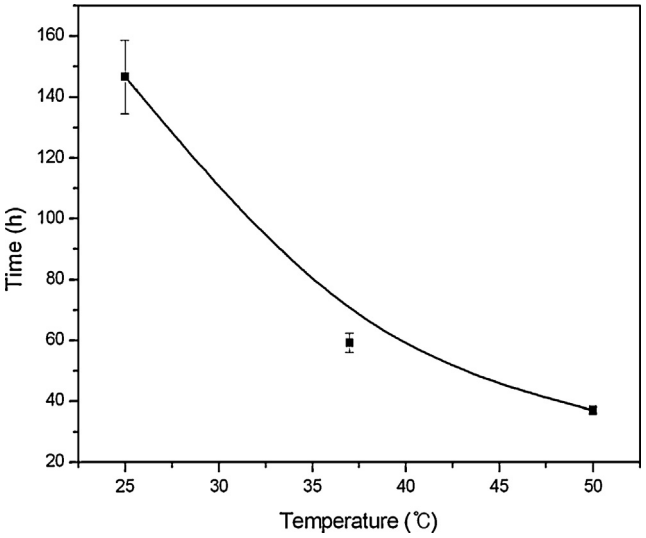

Fig. 1. Change in gelation time of pure SF aqueous solution with temperature.

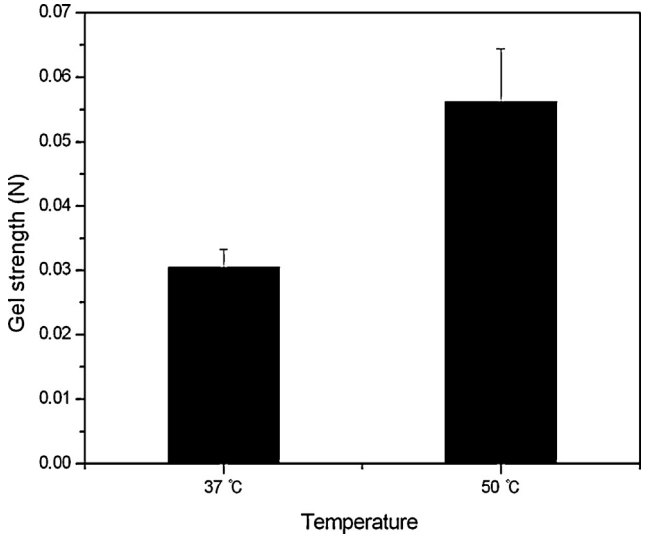

Fig. 3. Gel strength of SF hydrogel with temperature.

2.6. Characterization

The FT-IR spectra of the pure SF and SF/MC hydrogels were obtained by an Avatar 330 spectrometer (Thermo Nicolet) at a resolution of 2 cm^{-1}. A custom-made chamber was also used for the time-resolved measurements of the IR spectra of the SF gel samples. The viscosity of an SF/MC solution was measured using a Vibro Viscometer (SV-10, A&D Korea Ltd.) until the gelation was completed. A scanning electron microscope (JSM-7000F Beam Draw, JEOL, Japan) was used to investigate the morphology of the SF gels after freeze-drying. The compressive strength of the SF/MC hydrogels was measured using a texture meter (TA-XT2i, Stable Microsystems, Surrey, UK) equipped with a stainless-steel probe (diameter, 5 mm). Measurements were conducted with a penetration length of 3.0 mm, a measuring velocity of 1 mm/s, and a compressive force of 0.05 N.

3. Results and discussion

3.1. Gelation of SF aqueous solution

Fig. 1 shows the change in gelation time of pure SF aqueous solution with respect to temperature. The gelation time of SF aqueous solution decreased with increasing temperature. The hydrogelation of SF is accompanied by a conformational transition from a random coil structure to a β-sheet structure in the sol. A conformational transition from a random coil structure to a β-sheet structure was observed, and the formation of a β-sheet structure in the hydrogel was confirmed by time-resolved FT-IR spectra, as described in Section 3.3.

The morphology of SF hydrogels was observed by SEM after freeze-drying at −80 °C. Fig. 2 shows the SEM images of the freeze-dried SF hydrogels prepared at 37 °C and 50 °C. SF hydrogel showed sponge-like structure with interconnected pores, regardless of temperature. Pore sizes in the dried SF hydrogels decreased as the temperature increased with the same SF concentration. This could be explained by the increase in intermolecular hydrophobic interaction of SF molecules with temperature, resulting in the decrease in pore size. The compressive strength of SF hydrogels increased with increases in temperature (Fig. 3). At the same concentration, SF hydrogels prepared at a higher temperature showed higher gel strength as a result of the decreased pore size.

3.2. Gelation of SF/MC solution

The time-resolved measurements of IR absorption bands provided a useful means of monitoring the structural changes of SF as a function of gelation time (Huang et al., 2013; Shang et al., 2011;

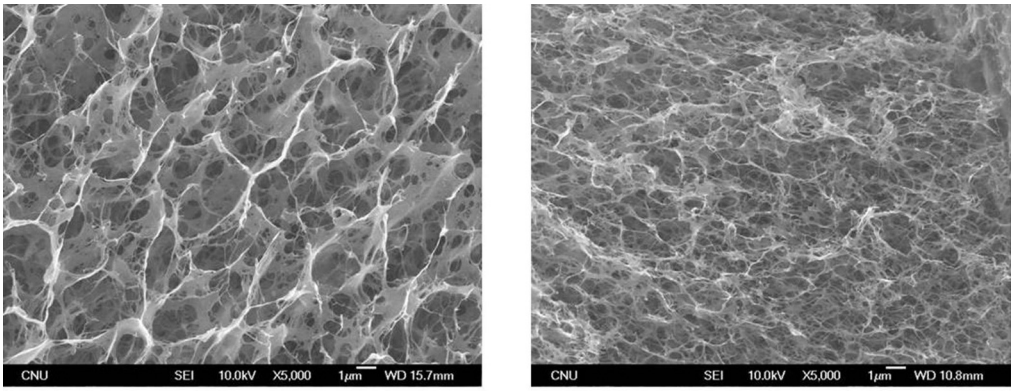

Fig. 2. SEM images of pure SF hydrogel at (a) 37 °C and (b) 50 °C (×5000).

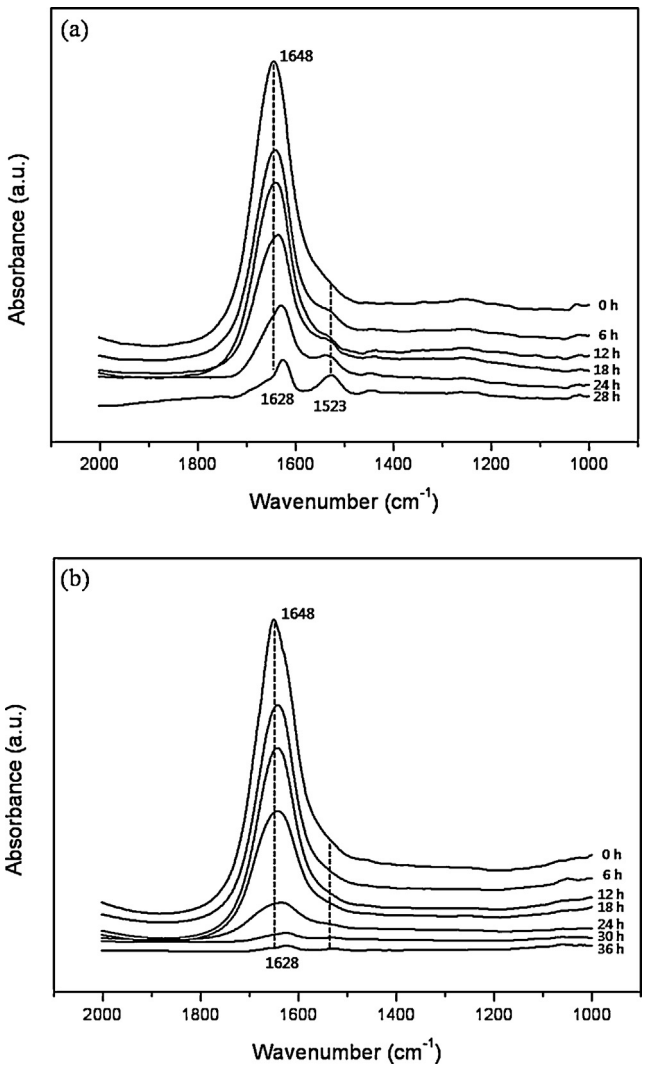

Fig. 4. FT-IR spectra change of pure (a) SF and (b) SF/MC(50/50) solution during gelation at 50 °C.

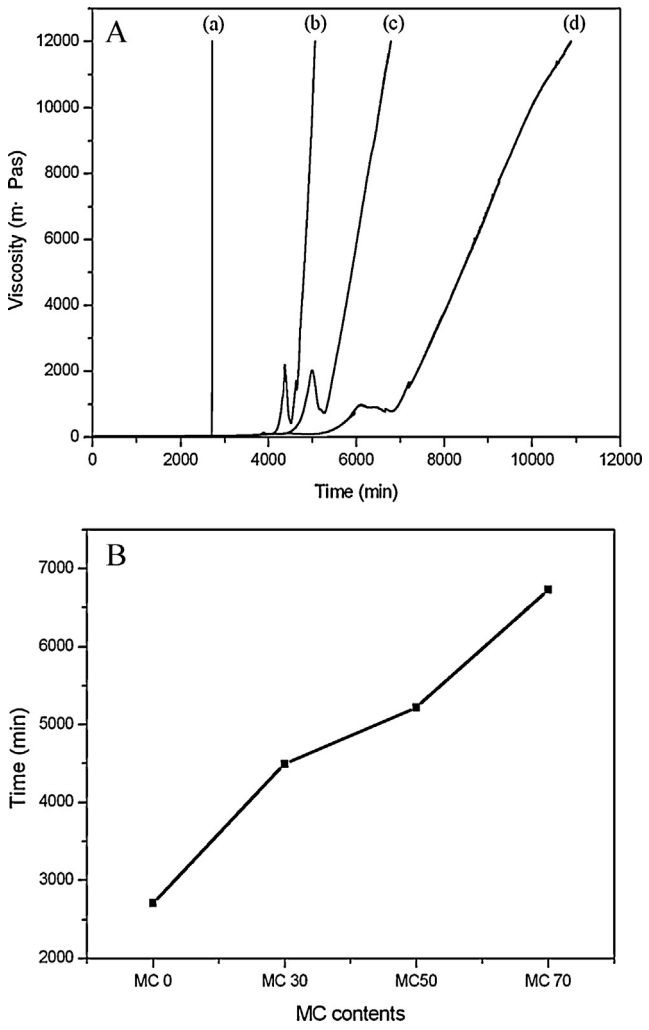

Fig. 6. (A) Viscosity data of SF/MC hydrogel; MC contents (a) 0%, (b) 30%, (c) 50%, and (d) 70%. (B) Gelation time determined from the viscometer.

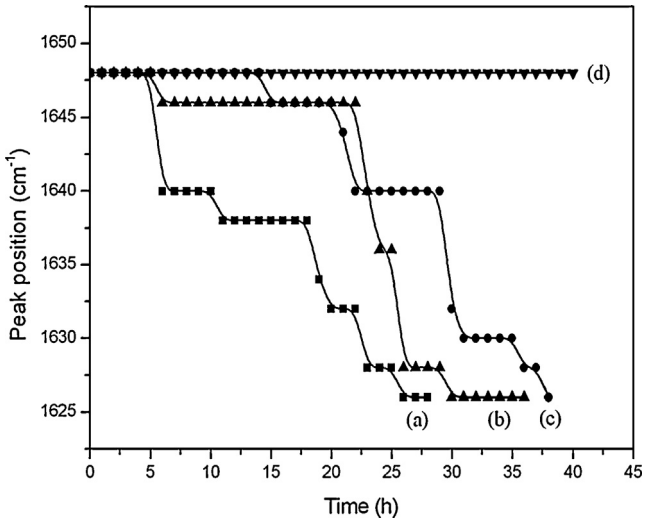

Fig. 5. Changes in the peak position of the amide I band (β-sheet conformation) of SF/MC solution: SF/MC ratio (a) 100/0, (b) 70/30, (c) 50/50, and (d) 30/70.

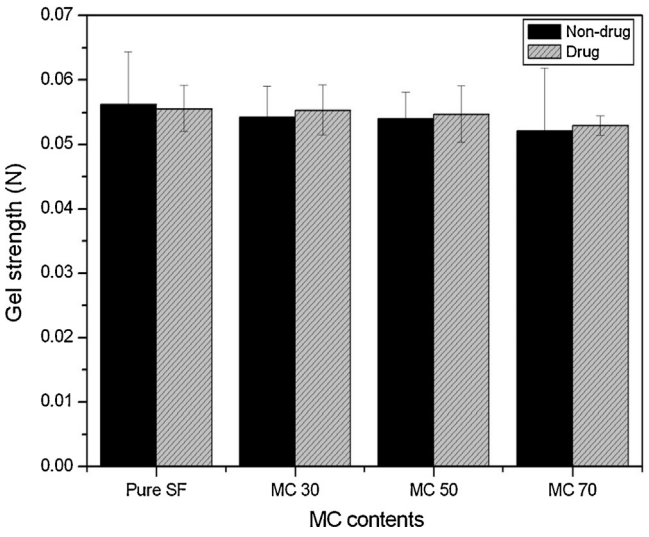

Fig. 7. Gel strength of SF/MC hydrogels with different MC contents.

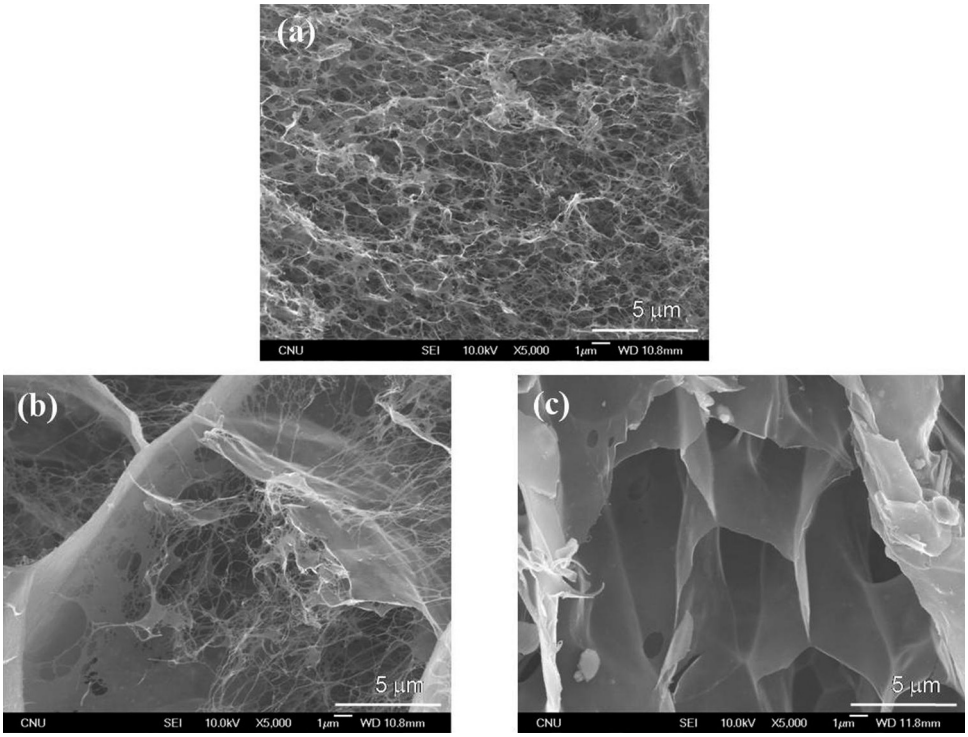

Fig. 8. SEM images of (a) pure SF gel, (b) SF/MC hydrogel (MC contents, 30%), and (c) SF/MC hydrogel (MC contents, 70%) (×5000).

Yoshioka & Tashiro, 2004). Changes in the characteristic absorption peak of the amide I and II bands of SF hydrogel during gelation at 50 °C are shown in Fig. 4a. The characteristic absorption peak of the pure SF aqueous solution were observed at 1648 cm^{-1} (amide I), which can be attributed to the random coil conformation (Fig. 4a). Interestingly, this band was shifted to 1628 cm^{-1} (amide I) during gelation, with the clear appearance of a peak at 1523 cm^{-1}, which is indicative of structural changes in the SF from the random coil conformation to the β-sheet conformation. This transition was also observed in the SF/MC solution (50/50, v/v), as shown in Fig. 4b. These results confirm that the structural change of SF from random coil structure to β-sheet structure was not inhibited by the addition of MC.

Fig. 5 presents the change in the peak position at 1548 cm^{-1} (amide I band) of the SF hydrogel with gelation time as a function of SF/MC ratio at 50 °C. Considering that the gelation starts with an abrupt change in peak position at 1548 cm^{-1}, the gelation time of SF was increased as the MC content increased up to 50%. The shift rate in the peak position of the amide I band increased as the MC content in the SF/MC mixture increased. The times to reach the ultimate peak position (1523 cm^{-1}) were lengthened from 26 h to 36 h as the MC content increased from 0% to 50% (Fig. 5). SF molecules were hydrated with a large amount of water in the solution state. By dehydration, SF molecules start to interact with each other, and thus form physical crosslinks, indicating conformational change from random coil structure to β-sheet structure (Shang, Zhu, & Fan, 2013). MC forms thermo-reversible hydrogel at 50 °C, and gel-to-sol transition occurs at below that temperature. It is known that hydrophobic interactions by substituted methyl groups in the cellulose backbone play an important role in the gelation of MC. The dehydration rate of MC was faster than that of SF. Subsequently, SF molecules were surrounded by more water molecules from the MC gelation process, resulting in increased gelation time of the SF.

The gelation time of SF/MC solutions was measured by the change in viscosity. Fig. 6A shows the change in viscosity of SF/MC solution with MC contents. The viscosity of the SF solution started to dramatically increase due to the gelation of the SF macromolecular chains. The gelation time was determined from the tangent line of the viscosity curve. Fig. 6B shows the gelation time determined from viscosity data as a function of MC content in the SF/MC solution. The gelation time of SF in SF/MC solution was increased with increasing MC content. Fig. 7 shows the gel strength of the SF/MC hydrogel containing different MC contents, with or without 5-aminosalicylic acid. The gel strength of pure SF hydrogel was 0.056 N, and did not change much with increasing MC content. Also, the addition of 5-aminosalicylic acid did not affect the gel strength of SF/MC hydrogels. As described previously, MC forms a thermo-reversible gel, which was changed to a sol state at below 50 °C. Interestingly, SF/MC hydrogel was maintained even at room temperature, without a decrease in gel strength. In order to investigate the maintenance of SF/MC hydrogel at lower temperature, the morphology of freeze-dried hydrogels was observed. Fig. 8 shows the morphology of freeze-dried SF/MC hydrogels. In a pure SF hydrogel, fibrillar network structures with small pores were observed. In contrast, SF/MC hydrogel with higher MC content (70%) showed mainly honeycomb-like structure with large pores. In the case of SF/MC (70/30) hydrogel, the fibrillar networks of SF were combined with the honeycomb-like structure. It seems that the two different network structures were physically connected to each other (Fig. 8b). This indicates that the combined gel structure supported the strength of the SF/MC mixed gel.

3.3. Drug release behavior of SF and SF/MC hydrogels

The drug release of SF hydrogel was evaluated in 2-D and 3-D conditions using 5-aminosalicylic acid a model compound. The drug release in transdermal patches or wound dressings may be similar to 2-D condition. Fig. 9a presents the release profile of 5-aminosalicylic acid in the SF hydrogel evaluated in 2-D or 3-D at 37 °C. At 48 h, the % release of 5-aminosalicylic acid was found to be about 60% in 2-D, while the % release of 5-aminosalicylic acid was about 80% in 3-D. Also, a burst effect in the early stages was

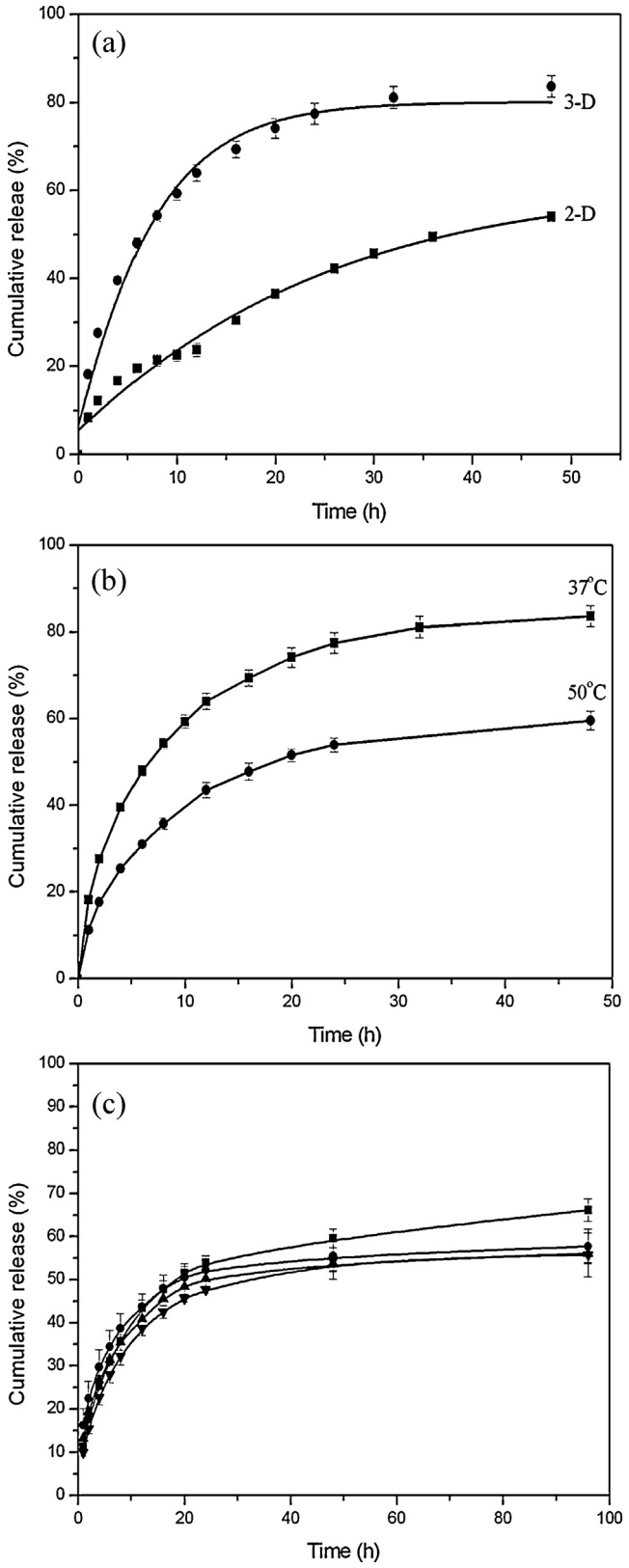

Fig. 9. Drug release profile of (a and b) SF and (c) SF/MC hydrogel in MC contents (■) 0%, (●) 30%, (▲) 50%, and (▼) 70%.

observed, which could have been due to the lack of interaction between hydrophobic SF molecules and 5-aminosalicylic acid, a hydrophilic drug.

The release of a drug from a hydrogel has been reported to be governed by several factors, such as the nature and molecular weight of the drug, the degree of crosslinking density, the pore size of the matrix, and the solvent type. Fig. 9b shows the drug release profiles of SF hydrogel prepared at 37 °C or 50 °C (3-D condition). The release (%) of 5-aminosalicylic acid from SF hydrogel prepared at 37 °C was faster than that from hydrogel prepared at 50 °C. At 48 h, the release (%) of 5-aminosalicylic acid from SF hydrogels at 37 °C and 50 °C were 80% and 55%, respectively. It seems that this difference in release patterns was closely associated with pore size, as described previously.

The extent of the initial burst release and duration of the drug release can be affected by the hydrophobicity of the drug, the molecular weight of the drug, the intermolecular interactions between drugs and polymers, and the degradation rate of the polymer (Moon, Ko, Park, Joo, & Jeong, 2012). Fig. 9c shows the release profile of 5-aminosalicylic acid in SF/MC hydrogel with different MC contents (50 °C, 3-D condition). The release (%) of 5-aminosalicylic acid in pure SF hydrogel was 65% at 96 h, whereas the release (%) of 5-aminosalicylic acid in SF/MC mixed gels was about 55%, regardless of MC content. This can be explained by the differences in polymer–drug interactions. MC molecules are more hydrophilic than SF molecules. 5-Aminosalicylic acid was expected to have a stronger interaction with MC molecules than SF molecules. It was concluded that the stronger interaction between MC and 5-aminosalicylic acid reduces the release rate of 5-aminosalicylic acid from the SF/MC mixed gel.

4. Conclusions

This study has demonstrated that the gelation time of SF/MC aqueous solutions was increased with the MC content, which also affected the drug release of the resultant mixed gels. From FT-IR spectra, the hydrogelation of SF and SF/MC solution was confirmed by the change in the amide I peak position, which represents random coil structure to β-sheet structure in the SF molecular chains. The gelation time of SF aqueous solution increased linearly with the MC content, because the gelation of MC molecules also occurred separately during the gelation of SF, thus inhibiting the transition of SF aqueous solution from random coil to β-sheet structure. In addition, the drug release of either SF or SF/MC hydrogels was studied using 5-aminosalicylic acid *in vitro*. In the pure SF hydrogel, 5-aminosalicylic acid was loaded into SF solution, and up to 60% and 80% was released at 48 h in 2-D and 3-D, respectively. The lower release rate of 5-aminosalicylic acid in SF/MC hydrogel than in SF hydrogel seemed to be caused by a higher interaction between MC and 5-aminosalicylic acid. This approach to controlling the sol–gel transition of SF hydrogel by the addition of MC may find useful applications in the design and tailoring of novel materials for biomedical applications, including wound dressings, drug delivery vehicles, and scaffolds for soft tissue engineering.

Acknowledgments

This work was supported by the National Research Foundation of Korea (2012035747).

References

Arisz, P. W., Kauw, H. J. J., & Boon, J. J. (1995). Substituent distribution along the cellulose backbone in O-methylcellulose using GC and FAB-MS for monomer and oligomer analysis. *Carbohydrate Research*, *271*, 1–14.

Ayutsede, J., Gandhi, M., Sukigara, S., Micklus, M., Chen, H. E., & Ko, F. (2005). Regeneration of *Bombyx mori* silk by electrospinning. Part 3: Characterization of electrospun nonwoven mat. *Polymer*, *46*, 1625–1634.

Cai, K., Yao, K., Cui, Y., Yang, Z., Li, X., Xie, H., Qing, T., & Gao, L. (2002). Influence of different surface modification treatments on poly(D, L-lactic acid) with silk fibroin and their effects on the culture of osteoblast in vitro. *Biomaterials*, *23*, 1603–1611.

Cai, K., Yao, K., Lin, S., Yang, Z., Li, X., Xie, H., Qing, T., & Gao, L. (2002). Poly(D,L-lactic acid) surfaces modified by silk fibroin: Effects on the culture of osteoblast in vitro. *Biomaterials*, *23*, 1153–1160.

Dinerman, A., Cappello, A. J., Ghandehari, H., & Hoag, S. W. (2002). Solute diffusion in genetically engineered silk-elastinlike protein polymer hydrogels. *Journal of Controlled Release*, *82*, 277–287.

Fuji, K., Takahashi, S., & Kinouchi, R. (2000). Preparation and properties of a novel sponge cake by combining rice flour with silk fibroin protein. *Japanese Society for Food Science and Technology*, *47*, 363–368.

Gil, E. S., Frankowski, D. J., Spontak, R. J., & Hudson, S. M. (2005). Swelling behavior and morphological evolution of mixed gelatin/silk fibroin hydrogels. *Biomacromolecules*, *6*, 3079–3087.

Hirrien, M., Chevillard, C., Desbrieres, J., Axelos, M. A. V., & Rinaudo, M. (1998). Thermogelation of methylcelluloses: New evidence for understanding the gelation mechanism. *Polymer*, *39*, 6251–6259.

Huang, H., Wu, J., Lin, X., Li, L., Shang, S., Yuen, M. C., & Yan, G. (2013). Self-assembly of polypyrrole/chitosan composite hydrogels. *Carbohydrate Polymers*, *95*, 72–76.

Jin, H. J., & Kaplan, D. L. (2003). Mechanism of silk processing in insects and spiders. *Nature*, *424*, 1057–1061.

Karageorgiou, V., Meinel, L., Hofmann, S., Malhotra, A., Volloch, V., & Kaplan, D. (2004). Bone morphogenetic protein-2 decorated silk fibroin films induce osteogenic differentiation of human bone marrow stromal cells. *Journal of Biomedical Materials Research Part A*, *71A*, 528–537.

Kim, U. J., Park, J., Li, C., Jin, H. J., Valluzzi, R., & Kaplan, D. L. (2004). Structure and properties of silk hydrogels. *Biomacromolecules*, *5*, 786–792.

Kundu, J., Poole-Warren, L. A., Martens, P., & Kundu, S. C. (2012). Silk fibroin/poly(vinyl alcohol) photocrosslinked hydrogels for delivery of macromolecular drugs. *Acta Biomaterialia*, *8*, 1720–1729.

Lee, K. Y., & Mooney, D. J. (2001). Hydrogel for tissue engineering. *Chemical Reviews*, *101*, 1869–1879.

Li, M., Lu, S., Wu, Z., Tan, K., Minoura, N., & Kuga, S. (2002). Structure and properties of silk fibroin–poly(vinyl alcohol) gel. *International Journal of Biological Macromolecules*, *30*, 89–94.

Lin, S. Y., Wang, S. L., Wei, Y. S., & Li, M. J. (2007). Temperature effect on water desorption from methylcellulose films studied by thermal. FT-IR micro spectroscopy. *Surface Science*, *601*, 781–785.

Lv, Q., Hu, K., Feng, Q., & Cui, F. (2008). Fibroin/collagen hybrid hydrogels with crosslinking method: Preparation, properties, and cytocompatibility. *Journal of Biomedical Materials Research Part A*, *84*, 198–207.

Mandal, B. B., Kapoor, S., & Kundu, S. C. (2009). Silk fibroin/polyacrylamide semi-interpenetrating network hydrogels for controlled drug release. *Biomaterials*, *30*, 2826–2836.

Matsumoto, A., Chen, J., Collette, A. L., Kim, U. J., Altman, G. H., Cebe, P., & Kaplan, D. L. (2006). Mechanisms of silk fibroin sol–gel transitions. *Journal of Physical Chemistry B*, *110*, 21630–21638.

Min, B. M., Jeong, L., Nam, Y. S., Kim, J. M., Kim, J. Y., & Park, W. H. (2004). Formation of silk fibroin matrices with different texture and its cellular response to normal human keratinocytes. *International Journal of Biological Macromolecules*, *34*, 223–230.

Min, B. M., Lee, G., Kim, S. H., Nam, Y. S., Lee, T. S., & Park, W. H. (2004). Electrospinning of silk fibroin nanofibers and its effect on the adhesion and spreading of normal human keratinocytes and fibroblasts in vitro. *Biomaterials*, *25*, 1289–1297.

Moon, H. J., Ko, D. Y., Park, M. H., Joo, M. K., & Jeong, B. (2012). Temperature-responsive compounds as in situ gelling biomedical materials. *Chemical Society Review*, *41*, 4860–4883.

Motta, A., Migliaresi, C., Faccioni, F., Torricelli, P., Fini, M., & Giardino, R. (2004). Fibroin hydrogels for biomedical applications: Preparation, characterization and in vitro cell culture studies. *Journal of Biomaterials Science Polymer Edition*, *15*, 851–864.

Motta, A., Migliaresi, C., Lloyd, A. W., Denyer, S. P., & Santin, M. (2002). Serum protein absorption on silk fibroin fibers and films: Surface opsonization and binding strength. *Journal of Bioactive and Compatible Polymers*, *17*, 23–35.

Padamwar, M. N., & Pawar, A. P. (2004). Silk sericin and its applications: A review. *Journal of Scientific & Industrial Research*, *63*, 323–329.

Park, W. H., Ha, W. S., Ito, H., Miyamoto, T., Inagaki, H., & Noishiki, Y. (2001). Relationships between antithrombogenicity and surface free energy of regenerated silk fibroin films. *Fibers and Polymers*, *2*, 58–63.

Putthanarat, S., Zarkoob, S., Magoshi, J., Che, J. A., Eby, R. K., Stone, M., & Adams, W. W. (2002). Effect of processing temperature on the morphology of silk membranes. *Polymer*, *43*, 3405–3413.

Sakabe, H., Ito, H., Miyamoto, T., Noishiki, Y., & Ha, W. S. (1989). In vivo blood compatibility of regenerated silk fibroin. *Sen-i Gakkaishi*, *45*, 487–490.

Santin, M., Motta, A., Freddi, G., & Cannas, M. (1999). In vitro evaluation of the inflammatory potential of the silk fibroin. *Journal of Biomedical Materials Research*, *46*, 382–389.

Shang, S., Zhu, L., & Fan, J. (2011). Physical properties of silk fibroin/cellulose blend films regenerated from the hydrophilic ionic liquid. *Carbohydrate Polymers*, *86*, 462–468.

Shang, S., Zhu, L., & Fan, J. (2013). Intermolecular interactions between natural polysaccharides and silk fibroin protein. *Carbohydrate Polymers*, *93*, 561–573.

Vos, P., Bucko, M., Gemeiner, P., Navratil, M., Svitel, J., & Faas, M. (2009). Multiscale requirements for bioencapsulation in medicine and biotechnology. *Biomaterials*, *30*, 2559–2570.

Wang, X., Kluge, J. A., Leisk, G. G., & Kaplan, D. L. (2008). Sonication-induced gelation of silk fibroin for cell encapsulation. *Biomaterials*, *29*, 1054–1064.

West, J. L., & Hubbell, H. A. (1995). Photopolymerized hydrogel materials for drug delivery applications. *Reactive Polymers*, *25*, 139–147.

Wu, X., Hou, J., Li, M., Wang, J., Kaplan, D. L., & Lu, S. (2012). Sodium dodecyl sulfate-induced rapid gelation of silk fibroin. *Acta Biomaterialia*, *8*, 2185–2192.

Yao, J., Masuda, H., Zhao, C., & Asakura, T. (2002). Artificial spinning and characterization of silk fiber from *Bombyx mori* silk fibroin in hexafluoroacetone hydrate. *Macromolecules*, *35*, 6–9.

Yoo, M. K., Kweon, H. Y., Lee, K. G., Lee, H. C., & Cho, C. S. (2004). Preparation of semi-interpenetrating polymer networks composed of silk fibroin and poloxamer macromer. *International Journal of Biological Macromolecules*, *34*, 263–270.

Yoshioka, A., & Tashiro, K. (2004). Solvent effect on the glass transition temperature of syndiotactic polystyrene viewed from time-resolved measurements of infrared spectra at the various temperatures and its simulation by molecular dynamics calculation. *Macromolecules*, *37*, 467–472.